Understanding the Invar Effect

RECENT PROGRESS

E.F. Wassermann

Tieftemperaturphysik, Universität Duisburg, Germany

The invar effect has intrigued solid state physicists ever since the discovery by Ch.E. Guillaume in 1897 that ferromagnetic, face centred cubic FeNi alloys with compositions close to $Fe_{65}Ni_{35}$ displayed almost constant — ''invariant'' — thermal expansion over a wide range of temperatures near room temperature. Guillaume was honoured with the Nobel Prize for Physics in 1920 for the discovery, and for that of temperature-independent elastic behaviour in FeNiCr (Elinvar) alloys. In spite of numerous attempts, the origins of the effect have never been fully understood so it remains to this day a challenging problem in solid state magnetism.

Invar and Elinvar-type alloys found widespread application soon after their discovery. Invar materials such as the classical FeNi alloys, ternary alloys of FeNiCo (Super Invar) or FeCoCr (Stainless Invar), which meet the need of dimensional stability with a varying temperature, are used in bimetal devices, precision tools and instruments, laser sources, lead frames for integrated circuits, and seismographic devices, to name but a few uses. Elinvar materials such as FeNiCr, or quarternary alloys of the system FeNiCoCr (Super Elinvar, Cobalt Elinvar) satisfying the requirement for elastic stability with temperature, find their main applications in time-recording instruments, in reeds, reed relays, and delay lines. Best-known, and once the most important application that is presently experiencing a certain revival, is the use of antiferromagnetic (AF) FeCrMn Elinvar as a hair spring and construction material for ''antimagnetic'' wrist watches.

In the field of basic research on magnetism, the widespread and continuous interest in Invar derives from two main reasons. First, the observation of invar-like anomalies are by no means tied to ferromagnetic (FM) alloys with a face centred cubic (fcc) structure. There are AF Invar alloys, and invar properties are also found in materials with body centred cubic (bcc), hexagonal or even amorphous structures, as well as in rare earth (RE) — transition metal compounds with a Laves phase structure (*e.g.* $RECo_2$, $REMn_2$) or compounds such as the recently discovered hard ferromagnet $Fe_{14}Nd_2B$. We know today a key point is that the systems are rich in at least one (but as we shall see, specific) 3d-transition element component. There are neither purely 4f, 5f nor insulating Invar alloys. The invar effect appears to be a problem of itinerant 3d-magnetism. Second, the anomaly in the thermal expansion is only one among many such anomalies. The list of anomalous physical properties of invar materials includes the temperature dependence of the lattice constant, heat capacity, magnetization, pressure dependence of the magnetization and of Curie (Néel) temperatures, spontaneous volume-magnetostriction at both low and high temperatures, and the thermal dependence of high field susceptibility and of elastic constants, as well as of Young's and bulk moduli.

The list demonstrates the richness of the invar effect as well as the complexity incorporated in it. We have recently reviewed and outlined the spectrum of properties [1] and the proceedings of a recent symposium [2] present a comprehensive overview.

Early Efforts

Much effort has been invested in accounting for the invar phenomenon theoretically and more than 20 different models have been published. The early local models stressed metallurgical and/or magnetic inhomogeneity since in the archetypical invar system FeNi, magnetovolume effects reach a maximum in a composition range where a strong deviation of the average magnetic moment (or magnetization) from the Slater-Pauling curve is observed. A structural transition from the fcc γ-phase to the bcc α-phase arises at the same time.

The subsequent observation of the invar effect in FM ordered Fe_3Pt, a system which shows neither mixed magnetic behaviour nor a deviation of the moment from the Slater-Pauling curve (but lies close to a γ-α transition) meant all the local models came into doubt. Homogeneous models based on the concept of weak itinerant ferromagnetism gave some progress in understanding Invars, but they failed to give an exact description of all the properties for the wide variety of systems listed above. The problem of correctly describing electronic and phononic features arising simultaneously remained largely unresolved.

Moment-Volume Instabilities

Recent progress towards a new theoretical understanding of Invars has been made *via* self-consistent band structure investigations within the local density approximation using the fixed spin moment (FSM) method [3]. The total energy of an alloy is calculated as a function of both the magnetic moment M and the atomic volume V to give so-called binding energy surfaces $E(M, V)$. Calculations have so far only been carried out for ordered structures. They essentially give the correct answers since the order-disorder transition, although playing a role, is not of crucial importance for understanding the invar effect.

We show in Fig. 1 examples of recent results of FSM calculations for ordered phases in the FeNi system [4]. Constant energy contours with a difference of 1 mRy (equivalent to $\approx$ 150 K) are projected onto the moment-volume plane. For Fe_3Ni which has a composition close to the archetype $Fe_{65}Ni_{35}$ Invar, additional contours (dashed lines) are given for a difference of 0.5 mRy. According to these results, pure fcc Fe is non-magnetic (NM) because the minimum in $E(M, V)$ lies on the abscissa, in contrast to work by other authors [2] predicting a metastable magnetic state for Fe at an expanded volume. The difference between these two results depends on details of the theoretical assumptions which will not be discussed. Moreover,

Professor E.F. Wassermann heads the Laboratory for Experimental Low Temperature Physics at the University of Duisburg, Germany. He studied physics at the Hilsch Institute, University of Göttingen and spent several years as a postdoc at Northwestern University, Illinois, USA before taking up an academic appointment in 1970 at the RWTH, Aachen.

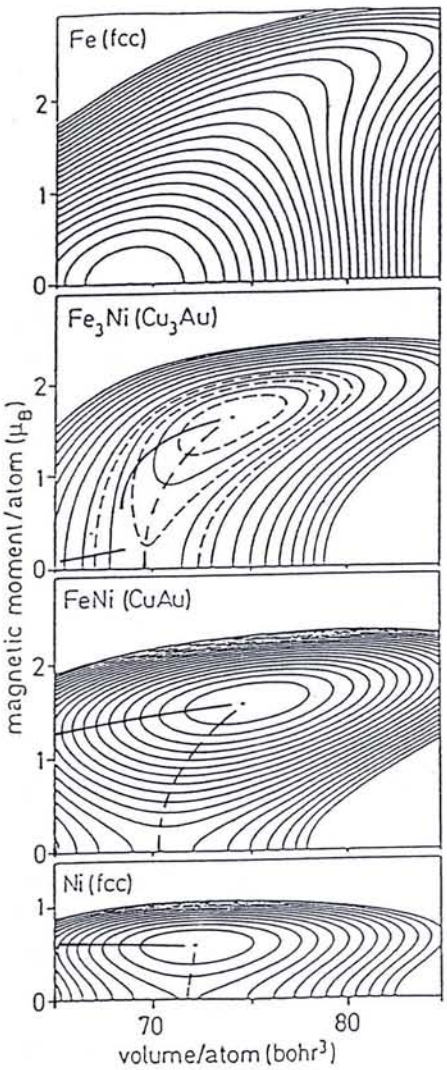

Fig. 1 — Constant energy contours projected onto the magnetic moment-volume plane as calculated with the fixed spin moment (FSM) by Mohn et al. [4] for the FeNi alloy series. The moment is give in units of the Bohr magneton μ_B and all data points are plotted on the same scale and all quantities are normalized to one atom per unit cell. The distances between contour lines is 1 mRy (≈ 150 K) with additional dashed contours at 0.5 mRy separations for ordered Fe_3Ni. The zero external field solutions ($H = dE/dM = 0$: full lines) and zero pressure solutions ($P = -dE/dV = 0$: dashed lines) are also shown. Note that pure fcc Fe, which is not stable in nature, is non-magnetic, while Ni and ordered FeNi are ferromagnets, as expected. Ordered Fe_3Ni, which is also not stable in nature but has a composition close to $Fe_{65}Ni_{35}$ (Invar), shows an instability of the moment with respect to small changes in the volume (moment-volume instablity: discontinuous full line).

comparison with experiment is difficult, since pure fcc Fe can only be stabilized as small, coherent, AF precipitates in *e.g.*, a Cu matrix.

On adding Ni to Fe, we see from Fig. 1 that a FM state develops (starting near Fe_3Ni) and becomes progressively more stable towards FeNi. Pure Ni is a stable ferromagnet as expected. We also plot in Fig. 1 the zero field solutions ($H = dE/dM = 0$: full lines) and zero pressure solutions ($p = -dE/dV = 0$: dashed lines) for Fe_3Ni, FeNi and Ni. According to these results, the moments in FeNi and pure Ni are stable and the NM state can only be reached experimentally at technically unrealistic elevated pressures.

The behaviour is different in Fe_3Ni, where the moment *versus* volume curve (full line in Fig. 1) drops discontinuously but parallel to the decrease in the zero pressure curve. This is the *key result* in a new understanding of the invar effect because it implies that in Fe_3Ni the moment is instable with respect to changes in volume. Thus, with increasing temperature or pressure, transitions from the so-called high spin state (with large magnetic moment and large atomic volume) into a low spin or non-magnetic state (with small or zero moment and small atomic volume) are possible, compensating for the "normal" thermal expansion of the lattice.

A similar moment-volume instability has also been found in total energy calculations for Fe_3Pt following the FSM method [5]. The validity of these theoretical findings has recently been confirmed by low temperature Mössbauer measurements made on $Fe_{68.5}Ni_{31.5}$ under pressure, and on ordered as well as disordered $Fe_{72}Pt_{28}$ [2]. Although the absolute values of the experimentally determined moments differ somewhat from theoretically predicted values, it is out of question that moment-volume instabilities form the basis for the occurrence of the invar effect.

Instabilities as a Function of *e/a*

In Fig. 2 are plotted the energy differences, $\Delta E = E_{NM}$-E_{FM} versus the electron concentration per atom *e/a* (counting 3d and 4s electrons) as given by Fig. 1 and reported in the literature (see [1-4] for details) by various authors using different computational methods. For fcc Fe, the NM state forms the ground state so that $\Delta E < 0$. The figure also plots a data result for disordered $Fe_{65}Ni_{35}$ (full dot) as well as for ordered Fe_3Pt (ΔE = 1.2 mRy [5]: triangle). A linear interpolation of all the data in Fig. 2 results in the shaded area.

While there is some uncertainty in the absolute theoretical values for ΔE, the data in Fig. 2 shows a general trend of ΔE *(e/a)* which can be used as the basis for an overall understanding of magnetic behaviour, magnetovolume effects and structural phase transitions, not only in FeNi but in all fcc 3d-alloy systems. We can in fact make the following statements:

1) For *e/a* around 9, the energy difference ΔE between the FM and NM states is large and positive (10-15 mRy). The critical pressure p_c ($= -2\,\Delta E/\Delta V$) for the transformation from the FM to the NM state is also large [4]. The systems are pure ferromagnets and are expected to exhibit either little or no magnetovolume effect.

2) In the range $8.5 \leq e/a \leq 8.7$, the energy difference ΔE is still positive, *i.e.*, the systems are ferromagnets, but absolute values of ΔE and p_c are small. The systems therefore show moment-volume instabilities equivalent to the occurrence of the invar effect.

3) With a further reduction in the electron concentration into the range *e/a* = 8.3–8.5, two different cases can be distinguished:
i) Both ΔE and p_c approach zero, which would lead to even larger magnetovolume effects than in the invar range.

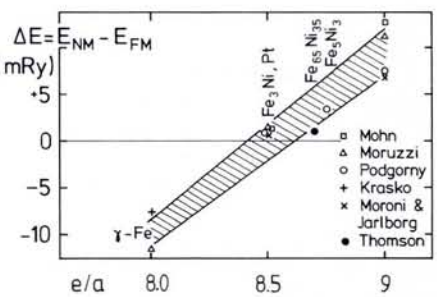

Fig. 2 — Energy differences $\Delta E = E_{NM} - E_{FM}$ between the non-magnetic (NM) and ferromagnetic (FM) instability states (see Fig. 1) as a function of the electron concentration per atom e/a. Data are taken from total energy calculations by different groups of workers (see [1-7]) using various theoretical models for fcc γ-Fe, Fe_3Ni and Fe_3Pt (with a Cu_3Au structure), disordered $Fe_{65}Ni_{35}$ (full dot), ordered Fe_5Ni_3 (face centred tetragonal super-cell), and ordered FeNi (CuAu structure). Linear interpolation results in the hatched area. For $8.5 \leq e/a \leq 8.7$, where ΔE is on the order of 1-2 mRy, we theoretically predict the occurrence of moment-volume instabilities (see Fig. 1, panel for Fe_3Ni) and observe experimentally the invar effect.

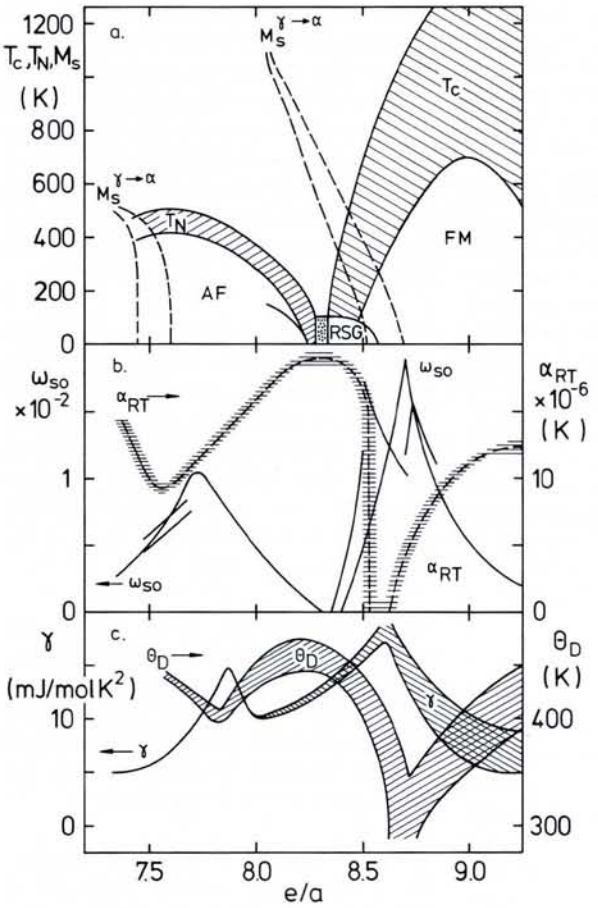

Fig. 3 — Various experimentally determined physical quantities as a function of the electron concentration per atom e/a for fcc alloys in the 3d-series (binary systems FeMn, FeCo, FeNi, FePt, FePd; ternary systems FeNiCr, FeNiMn, FeNiCo). Data points are omitted for clarity (see [1] for details) and only hatched areas in which experimental data points lie are shown.

a) Curie temperature T_c for ferromagnets, Néel temperatures for antiferromagnets, re-entrant spin glass range and pure spin glass range (dotted) versus e/a. Validity ranges of the martensite start temperatures for structural transitions from the fcc γ-phase to the bcc α-phase, $M_s^{\gamma-\alpha}(e/a)$ are also given.

b) Spontaneous volume magnetostriction extrapolated to zero temperature, $\omega_{SO} = (\Delta V/V)_{T\to 0}$ and thermal expansion coefficient at room temperature $\alpha_{RT} = [d(\Delta l/l)/dT]_{T=300\,K}$ versus e/a. ω_{SO} reaches a maximum of ≈ 2% in the FM invar range around e/a ≈ 8.6–8.7, and α_{RT} becomes very small or zero at the same time. Note that a similar behaviour of ω_{SO} and α_{RT} is observed in the AF Invar range around e/a = 7.5–7.7.

c) Debye temperatures Θ_D and electronic γ-terms, both from specific heat measurements, versus e/a. In analogy with the behaviours of $\omega_{SO}(e/a)$ and $\alpha_{RT}(e/a)$ in Fig. 3b, note the softening of the lattice (decrease of Θ_D) and an increase in the electronic γ-term (proportional to the density of states) in both the FM and AF invar ranges.

However, the fcc lattice cannot tolerate a volume increase larger than ≈ 2% as observed in Invar so the systems undergo a structural phase transition from the dense packed fcc phase to the more open structure of the bcc phase (a martensitic transition, see below).

ii) Reducing *e/a* by alloying Mn (with *e/a* = 7) to, *e.g.*, FeNi leads to an increase in the lattice constants of the alloys owing to the large atomic volume of Mn. Magnetovolume effects are reduced as a result and the transitions in the range around *e/a* ≈ 8.6 are suppressed. Instead, since Mn atoms tend towards AF coupling, mixed exchange interactions occur and one observes either re-entrant (RSG) or pure spin (SG) glass order for *e/a* ≈ 8.3–8.5.

4) Antiferromagnetism is theoretically not yet correctly incorporated in the FSM calculations so that in the range *e/a* ≤ 8.3, for pure fcc Fe or even FeMn (*e/a* = 7.5) where $\Delta E(e/a)$ is negative (Fig. 1), the theoretical results do not describe the actual situation.

Finite temperature

We have so far ignored the fact that the invar effect arises at finite temperatures whereas the band structure calculations were carried out for temperature T = 0 K. Although finite temperature calculations are in their infancy [4], it is beyond dispute that the experimentally observed broad spectrum of physical anomalies in 3d-transition metal alloys at finite temperature also finds its origin in the existence of moment-volume instabilities. The physical nature of the excitations from the ground state in these systems is not yet fully understood. However, there are transverse spin fluctuations (spin waves as revealed by neutron scattering [1]) and longitudinal spin fluctuations coupled to fluctuations of the volume. The presence of these magnetoacoustic (''forbidden'') modes has recently been clearly demonstrated in neutron scattering experiments [2].

Comparison with Experiment

The validity of the four preceding statements (1-4) is readily proven by comparisons with experimental data. Fig. 3 plots various experimentally determined quantities as a function of *e/a* for the systems FeNi, FeCo, FeMn, FePt, FePd, FeNiCr, FeNiMn, and FeNiCo. Data points are omitted for clarity (they are reported elsewhere in detail [1]) and only hatched regions in which the experimental results lie are shown.

Fig. 3a gives the magnetic ordering temperatures (Curie temperatures T_c for the ferromagnets, Néel temperatures T_N for the antiferromagnets, glass temperatures T_g for the re-entrant and pure spin glasses) as well as the martensitic start temperatures $M_s^{\gamma\to\alpha}$ — discussed below — for the onset of structural transitions (dashed lines). In agreement with the statements, there is pure FM order present for *e/a* ≈ 8.6, pure itinerant SG order (dotted region) around *e/a* ≈ 8.3 and AF order for *e/a* ≥ 8.3. The spontaneous volume magnetostriction extrapolated to zero temperature, ω_{SO}, plotted in Fig. 3b peaks in the FM invar range around *e/a* ≈ 8.7 and in the AF invar range at *e/a* ≈ 7.7. Conversely, the thermal expansion coefficient at room temperature, α_{RT}, also plotted in Fig. 3b has minima when ω_{SO} reaches a maximum, and *vice versa*. Note further that around *e/a* = 8.3 in the spin glass regime, ω_{SO} vanishes and α_{RT} reaches values of almost 20 × 10^{-6} K^{-1}. It has been shown previously [1] that the maxima in ω_{SO} and minima in α_{RT} as a function of *e/a* are accompanied by maxima in $dT_{C,N}/dp$, the pressure dependence of the Curie (Néel) temperature (the data are not shown here).

As can be seen from Fig. 3c, the exaggerated magnetovolume effects in the 3d-alloy series are accompanied by a softening of the lattice. The Debye temperatures Θ_D as a function of *e/a* decrease around *e/a* = 8.7 and 7.7. Fig. 3c reveals at the same time that the α-terms of the electronic specific heat determined at low temperatures are only slightly enhanced with respect to ''normal'' behaviour, but clearly increase in the critical regions of *e/a*.

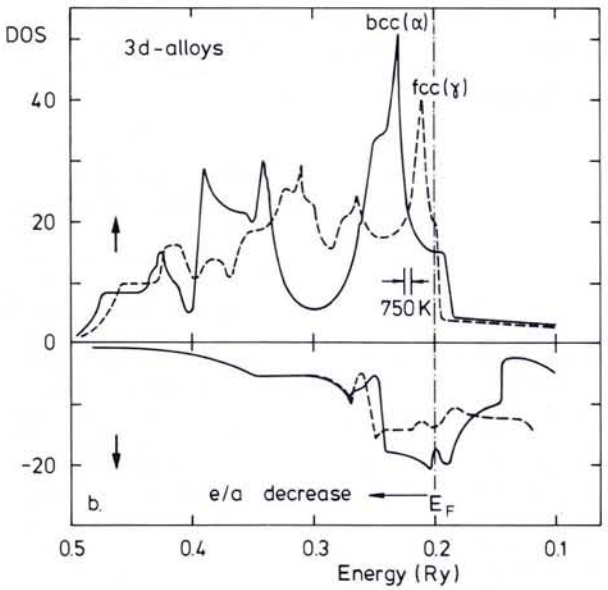

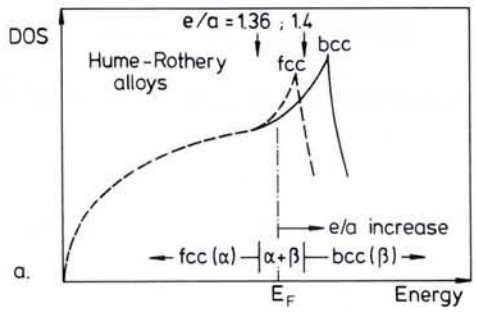

Fig. 4 — a, upper) Electronic density of states (DOS) versus energy for non-magnetic Hume-Rothery alloys such, e.g. brass (CuZn), with fcc (α) and bcc (ω) lattice structures (schematically). Note that on increasing the electron concentration, equivalent to a shift to the right of the Fermi energy E_F, these alloys undergo an fcc-bcc structural transition at an electron concentration of e/a ≈ 1.4 because for e/a ≥ 1.4, the bcc DOS is much larger than the fcc DOS, a feature that favours the stability of the bcc phase.
b, left) Spin split DOS for a ferromagnetic (FM) 3d-alloy with fcc (γ) or bcc (β) structures at the same atomic volume, $\Omega_{fcc} = \Omega_{bcc}$. Actual data for Mn taken from [6]. Note that in this case, using the same arguments as above, an fcc-bcc structural transition occurs when e/a decreases.

Martensitic Transitions

In the *e/a* range close to 8.6 (for T = 0 K), the FM alloys without Mn or Cr, namely FeNi, FePt, FePd, and FeNiCo, undergo a martensitic phase transition from a fcc to a bcc structure with the martensitic start temperatures $M_s^{\gamma\to\alpha}$ versus *e/a* shown in Fig. 3a (dashed lines). The experimental data also reveal that the same type of transition occurs for the AF alloys FeMn, FeNiMn and FeNiCr in the range around *e/a* ≈ 7.5, *i.e.*, at values below those where AF invar behaviour is observed. The fact that these structural transitions occur at certain, relatively well defined electron concentrations in the magnetic 3d-alloy series recall the Hume-Rothery rules (where an alloy changes structure at specific electron concentrations) that are well established for NM alloys. However, whereas the Hume-Rothery alloys (*e.g.* CuZn) undergo an fcc-bcc structural transition on increasing the electron concentration, the magnetic 3d-alloys undergo the same transition on decreasing the same parameter.

This difference can be reconciled in terms of a rigid band model by differentiating the electronic structures of the two classes of systems, as illustrated in Fig. 4. Fig. 4a shows the density of states (DOS) for NM Hume-Rothery alloys in the fcc and bcc phases as reported in textbooks. The DOS up to *e/a* = 1.36 in the fcc phase (for a given atomic volume $\Omega_{bcc} = \Omega_{fcc}$) is equal to the DOS in the bcc phase, but on **increasing** *e/a* (after passing through the α + β transition region) the systems are in the bcc phase for *e/a* ≥ 1.4 as the DOS is larger than for the fcc phase.

Fig. 4b shows typical DOS curves for FM 3d-elements (or alloys) in the fcc and bcc phases. We have chosen a spin split DOS as given in the literature [6] for pure Mn with $\Omega_{bcc} = \Omega_{fcc}$. However, other estimates of, for example, the total DOS [2, 3] can be used as well. The structural phase transition behaviour as a function of *e/a* for the 3d-series is readily understood from Fig. 4b. The sharp peak in the bcc DOS for these alloys lies at lower energies than the fcc peak so the systems undergo a fcc-bcc structural phase transition when the Fermi energy E_F moves from a position at the peak in the up-spin fcc DOS through the minimum into a another position at the peak in the up-spin bcc DOS. This movement of E_F (see arrow in Fig. 4b) takes place on **decreasing** the electron concentration. Total DOS results also reveal that the peak in the bcc DOS corresponds to *e/a* = 8.6, in agreement with the results of Fig. 3a for the occurrence of the γ-d transition in FM 3d-alloys. We have recently shown that the finite temperature behaviour (M_s increasing as *e/a* decreases, see Fig. 3a) can be understood using very similar arguments [7].

Conclusions

The latest types of band structure calculations predicting the occurrence of moment-volume instabilities in fcc systems such as Fe_3Ni and Fe_3Pt provide for a new understanding of the invar effect. They yield the basis for a general explanation of the broad spectrum of magnetovolume effects and structural transitions that have been observed in 3d-alloys on varying the electron concentration.

Further work is necessary to explain the dynamics of these instabilities (finite temperature spin and volume fluctuations) and to yield more insight into the properties of itinerant antiferromagnets. This could also lead to a better understanding of the heavy fermion systems, where moment-volume instabilities similar to those arising in the AF 3d-alloys are observed, albeit with magnetic moments as small as 0.05 μ_B and critical temperatures of the order of several Kelvin. Total energy calculations resembling those discussed for the Invar alloys, but with much higher resolutions, will perhaps soon be possible for these materials.

ACKNOWLEDGEMENTS

The present work was supported by the Deutsche Forschungsgemeinschaft within Sonderforschungsbereich 166 ("Structural and Magnetic Phase Transitions in Transition Metal Alloys"). The author thanks M. Acet, P. Entel, W. Pepperhoff, M. Podgórny and D. Wagner for valuable discussions.

REFERENCES

[1] Wassermann E.F. in *Ferromagnetic Materials*, Vol. V; Eds. P. Wolfarth and K.H. Buschow (North-Holland, Amsterdam, 1990) pp. 240-317.
[2] Proc. Int. Symp. on Magnetoelasticity and Electronic Structure of Transition Metals, Alloys and Films; *Physica B* **161** (1989).
[3] Williams A.R. *et al., J. Appl. Phys.* **53** (1982) 2019.
[4] Mohn P., Schwarz. K. and Wagner D., *Phys Rev. B* **43** (1991) 3318.
[5] Podgórny M., *Phys. Rev B* (1991) to be published.
[6] Fuster G. *et al., Phys. Rev B* **38** (1988) 423.
[7] Wassermann E.F., Acet M. and Pepperhoff W., *J. Magn. Mag. Mater.* **90 & 91** (1990) 126.